Ocean Sci., 21, 1487–1503, 2025
https://doi.org/10.5194/os-21-1487-2025

Ocean Science
Open Access

Extreme sensitivity of the northeastern Gulf of Lion (western Mediterranean) to subsurface heatwaves: physical processes and insights into effects on gorgonian populations in the summer of 2022

Claude Estournel[1], **Tristan Estaque**[2], **Caroline Ulses**[1], **Quentin-Boris Barral**[1], **and Patrick Marsaleix**[1]

[1]Université de Toulouse, LEGOS (CNES/CNRS/IRD/UT3), Toulouse, France
[2]Septentrion Environnement, Marseille, France

Correspondence: Claude Estournel (claude.estournel@cnrs.fr)

Received: 9 December 2024 – Discussion started: 17 December 2024
Revised: 20 March 2025 – Accepted: 2 April 2025 – Published: 24 July 2025

Abstract. In the summer of 2022, atmospheric conditions characterized by persistent anticyclonic anomalies caused an extreme marine heatwave in the western Mediterranean Sea. Time series of temperature profiles at various points along the northeastern coast of the Gulf of Lion (NW Mediterranean Sea) showed exceptional temperatures down to depths of 30 m, which led to massive mortality of benthic species. A hydrodynamic numerical simulation was used to analyze the physical processes responsible for this subsurface heatwave in a region where the climatology in summer is characterized by northerly winds inducing upwelling alternating with low winds. Firstly, the recurrence of heatwaves limited to the surface was demonstrated, triggered when upwelling stopped and warm water from the Northern Current intruded onto the shelf. More importantly, in August and early September 2022, two episodes of southerly and easterly winds of 8 to 10 m s^{-1} occurred. The oceanic response to these winds was an alongshore cyclonic current advecting warm water onto the shelf and a downwelling of this warm water to depths of the order of 30 to 40 m. A large part of the Gulf of Lion coast was warmed by these events. However, the northeastern part of the shelf, on either side of the city of Marseille, was by far the area most affected at depth due to the combination of the proximity of the warm surface waters of the Ligurian coast advected by wind-induced currents and the local acceleration of the wind by the continental topography, which intensifies the downwelling of these surface waters. These events are rare in summer, but their impact on the rich benthic ecosystems that characterize the region is dramatic and will only increase with the warming trend in surface waters, which is already close to 1 °C, as seen over the last decade.

1 Introduction

With global warming, the number, intensity, and duration of marine heatwaves (MHWs) are on the rise, and MHW events occur throughout the year (Fox-Kemper at al., 2021). Impacts on marine organisms are likely to be most marked in coastal areas. Benthic communities, being sedentary or having only limited mobility, are, indeed, particularly vulnerable to extreme temperatures (Lejeusne et al., 2010; Hughes et al., 2017; Garrabou et al., 2022) rather than to the exceedance of climatological values likely to occur throughout the year. This is the case for coral, with, for example, a bleaching threshold that is defined for the Hawaiian Islands to be when surface temperature exceeds the maximum monthly mean by 1° (Glynn and D'Croz, 1990). Therefore, when biological impacts are considered, it is summer heatwaves that should be particularly monitored.

While surface MHWs have been documented over several decades based on satellite SSTs (sea surface temperatures), in situ data documenting temperatures in the first few tens of meters below the surface are infrequent, and their spatial representativeness varies greatly from site to site, particularly in coastal areas, which are subject to unique dynamical processes due to the shallow depths and proximity to land (Schaeffer et al., 2023). On the one hand, irregularities in the coastline and submarine topography condi-

Published by Copernicus Publications on behalf of the European Geosciences Union.

tion horizontal alongshore and cross-shore exchanges; on the other hand, spatial variations in the wind (possibly related to continental relief) can generate localized coastal upwelling and downwelling depending on the orientation of the coastline relative to the wind direction. In contrast to upwelling, which counteracts the occurrence and intensity of heatwaves in the first few tens of meters of the water column (defined here as the subsurface) and is identifiable based on the SST, downwelling favors the penetration of warm surface water at depth, possibly beneath the stratified surface layer, and is generally not identifiable from the SST, especially as surface water can be cooled by air–sea heat fluxes (Schaeffer et al., 2023). Tracking coastal subsurface heatwaves is therefore impossible using surface information alone. As outlined by Schaeffer et al. (2023), the best proxy of subsurface temperature extremes appears to be wind anomalies since subsurface MHW events and years characterized by many subsurface MHW days are predominantly associated with wind-driven downwelling. Numerical models are the only way to document them at high spatial (horizontal and vertical) and temporal resolutions. However, their accuracy is a prerequisite when it comes to exceeding a tolerance threshold.

Since 1982, the Mediterranean SST has been warming at a mean rate of $\sim 0.35\,°C$ per decade (Pastor et al., 2020) compared with the global mean increase of 0.15 °C per decade (Fox-Kemper et al., 2021). For the 2010–2019 decade, Garrabou et al. (2022) showed an increase in warming for an average of seven coastal sites in the northwestern Mediterranean Sea, with values for the decade of 0.9 °C at 5 m and 0.6 °C at 35–40 m. Superimposed onto this long-term warming, several authors have noted an increased frequency, intensity, and duration of MHWs over the last 4 decades (Simon et al., 2022; Juza et al., 2022; Pastor and Khodayar Pardo, 2023) and an acceleration in recent years. Recently, an exceptionally long-lasting and intense MHW started in May 2022 (Martinez et al., 2023) and persisted until spring 2023 (Marullo et al., 2023). According to the latter authors, the intensity of this MHW was comparable to that of the 2003 event, which is the most intense case to have ever occurred in the last decades. The 2022 MHW was attributed to an atmospheric heatwave in western Europe due to a persistent anticyclonic anomaly (Guinaldo et al., 2023) exacerbated by climate change (Faranda et al., 2023). Never-before-recorded temperatures were observed at the surface of the western Mediterranean Sea during this summer (Guinaldo et al., 2023). In the Marseille area, east of the Gulf of Lion, temperatures exceeded 26 °C at 20 m for 4 d in August and exceeded 25 °C down to 30 m for 3 d in early September (see more details in Grenier et al., 2023; Estaque et al., 2023). Following these last authors, depths from 25 to 30 m were exposed for the very first time to temperatures above 25 °C, considered to be a potentially lethal acute heat stress threshold for benthic species (Crisci et al., 2011).

During the heatwaves of 1999 and 2003, large-scale ($>$ 1000 km coastline) mass mortality events affected numerous species of benthic invertebrates in the northwestern Mediterranean Sea (Bensoussan et al., 2010, and references herein), indicating that these species are living near their upper thermal thresholds. In the Parc National des Calanques, southeast of Marseille, high temperatures in the summer of 2022 had an unprecedented impact on the mortality of numerous species, especially for the red gorgonian *Paramuricea clavata* and the red coral *Corallium rubrum*, affecting depths down to 30 m (Estaque et al., 2023). Other emblematic species, such as sponges, have totally disappeared around Marseille at depths of down to 25 m, with only a few individuals surviving between 25 and 30 m (Grenier et al., 2023). The first sponge mortalities were recorded when temperatures exceeded 26 °C.

The aim of this article is to understand the interweaving of physical mechanisms from the large to the local scale at the origin of the summer 2022 subsurface heatwave, extreme in terms of its intensity and impacts in the region of Marseille. To achieve this, we use numerical modeling checked against a dense network for the top 40 m temperature measurements called T-MEDNet, which documents surface and subsurface heatwaves.

2 Main characteristics of the study site

The Gulf of Lion (Fig. 1) comprises a broad, crescent-shaped continental shelf enclosed between two straight coasts, the Ligurian coast to the northeast and the Catalan coast to the southwest, bordered by a narrow shelf and a steep continental slope, along which the Northern Current transports from northeast to southwest warm and low-salinity waters from the south of the western Mediterranean basin and originally from the Atlantic. Under certain meteorological conditions, the Northern Current splits into two branches, with the coastal branch entering the continental shelf along the coast (Barrier et al., 2016; Ross et al., 2016). These intrusions occur particularly under stratified conditions.

The northwestern Mediterranean Sea is a mosaic of contrasting hydrological situations due to bathymetric constraints and complex wind regimes. In the Gulf of Lion, the prevailing winds blow from land (north to northwest, referred to in the following as the northerly winds for simplicity's sake) and are channeled by orography, namely the Rhône Valley to the north, where the Mistral blows, and the passage between the Pyrenees and the Massif Central to the west, where the Tramontane blows. As a result, winds are much stronger in the Gulf of Lion than along the Catalan and Ligurian coasts. These northerly winds produce discontinuous coastal upwelling to the north of the zone, from around 3.5 to 5.8° E (Millot, 1990), leading to surface cooling in the summer that can exceed 10 °C in 1 to 2 d (Odic et al., 2022). Using criteria not detailed here, based on the temperature anomaly with respect to climatology and the cooling between 2 successive days, the frequency of these events

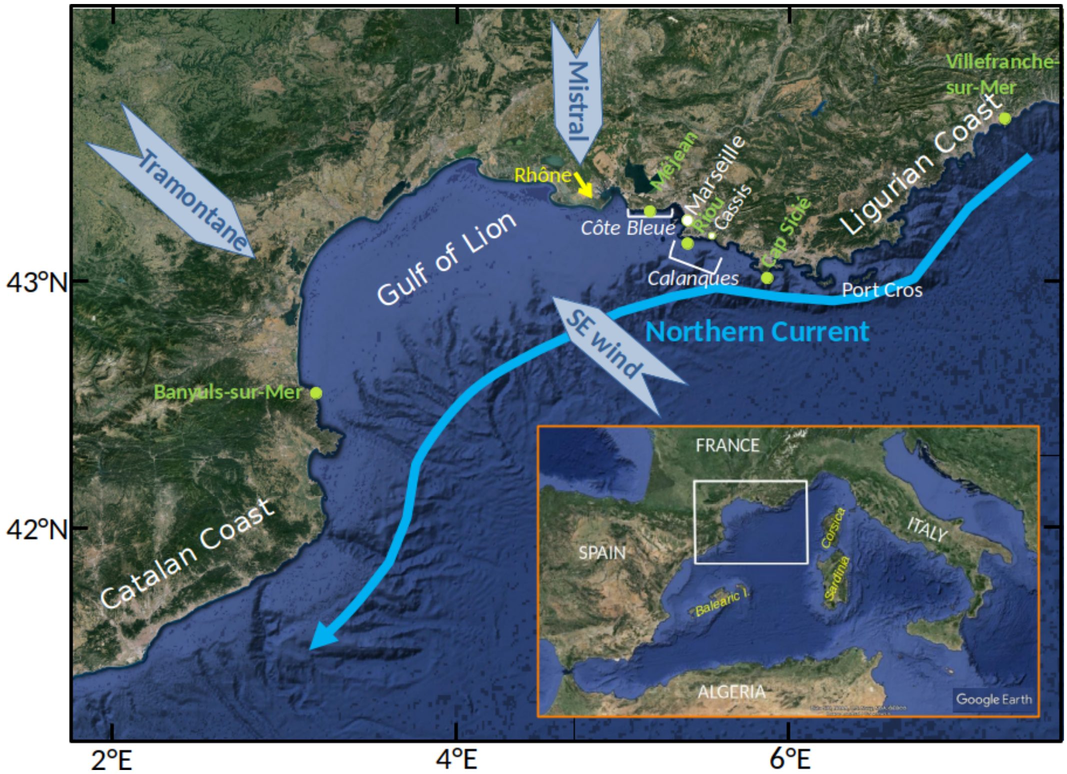

Figure 1. Location and topography of the study area (background map from © Google Earth). The prevailing Mistral and Tramontane winds, the southeastern wind, the Northern Current, and the regional branch of the general circulation are indicated, along with the different places named in the text. The solid green circles indicate the T-MEDNet observation points, namely Méjean, Banyuls-sur-Mer, and Villefranche-sur-Mer, on which comparisons with the model are focused, and Riou and Cap Sicié. The insert is a more general map of the western Mediterranean Sea, in which the area is indicated by a white rectangle.

near Marseille between 2012 and 2022 was 6.3 per summer on average (Quentin-Boris Barral, personal communication, 2024). For Tramontane, the western coast is, on the contrary, favorable to downwelling (Bensoussan et al., 2010; Odic et al., 2022), producing less variable surface temperatures but nevertheless presenting lower maximum values than in the east (Pairaud et al., 2014) due to an increase in wind intensity and frequency from east to west (Obermann-Hellhund et al., 2018) and a reduced influence of the warm Northern Current.

After these northerly winds, the second type of wind blows from southwest to southeast; however, locally, these winds are strongly influenced by the relief of the islands and the mainland, which can strongly modify their intensity and direction. They generally enter the Gulf of Lion from a direction that varies from east after following the Ligurian coast to southeast as they bypass Corsica and Sardinia and to south. In what follows, we will refer to these winds as southeasterly winds in accordance with several authors (e.g., Millot, 1990; Odic et al., 2022). Rare in July–August, their frequency and intensity then increase sharply to peak in October–November (Odic et al., 2022), when the wind is frequently accompanied by precipitation on the mainland, which can lead to flash flooding of rivers, possibly accompanied by significant material and human damage (Ducrocq et al., 2014; Drobinski et al., 2014). These winds, which can reach 25 m s^{-1} in winter, induce cyclonic circulation around the Gulf of Lion, with currents of several tens of centimeters per second, accompanied by intensified downwelling toward its southwestern tip due to the acceleration of currents linked to the narrowing of the continental shelf (Ulses et al., 2008; Mikolajczak et al., 2020).

The region around Marseille includes, to the east, the Parc National des Calanques, characterized by remarkable marine habitats (e.g., *Posidonia* meadows, coralligenous reefs, semi-dark caves, submarine canyons), 14 of which are considered to be rare and fragile (https://www.calanques-parcnational.fr/en/marine-habitats, last access: 16 July 2025) and which present a high risk of mass mortality associated with thermal stress for the red gorgonian (Pairaud et al., 2014), as well as for other cnidarians, numerous sponge species, bryozoans, and tunicates. To the west of Marseille, the Parc Marin de la Côte Bleue is another marine protected area, also hosting a great marine biodiversity similar to that found in the Parc National des Calanques but at relatively shallower depths. In this last area, the presence of remarkable mesophotic "giant"

Paramuricea clavata forests is particularly noticeable (Sartoretto et al., 2023).

3 Material and methods

We use a numerical simulation of the entire Mediterranean basin similar to that described in Estournel et al. (2021). The simulation is based on the 3D primitive-equation SYMPHONIE model (Marsaleix, 2024) described in Marsaleix et al. (2006, 2008) and in Damien et al. (2017), with the turbulence closure and convection parameterization detailed in Estournel et al. (2016). The VQS (vanishing quasi-sigma) vertical coordinate (Estournel et al., 2021) is used, with 60 levels. The horizontal resolution in the area of interest is around 1900 m, which may seem coarse for an application very close to the coast but has been proved to be sufficient to represent rapid temperature variations, as will be shown in Sect. 4.1, devoted to an evaluation of the simulations (Figs. 2 and 3). The model was initialized and forced in the Gulf of Cádiz (Atlantic Ocean) from daily operational oceanic analysis produced by MERCATOR OCEAN International. At the surface, it was forced based on the 12 hourly forecasts that follow the 00:00 and 12:00 UTC analyses of the ECMWF operational meteorological model. COARE bulk formulas were used to compute the turbulent air–sea fluxes. The simulation was initialized in May 2011. Comparisons with monthly satellite SSTs taken during two seasons, 6 and 7 years after model initialization, show a very good representation of large-scale features present in the whole basin but also of various smaller structures (Estournel et al., 2021).

At the coastal scale, the simulation is compared with T-MEDNet (https://t-mednet.org/, last access: 16 July 2025) observations taken at an hourly frequency every 5 m between 5 and 40 m with autonomous sensors fixed to the seabed rocky substrate. This region includes various T-MEDNet observation points stretching from the Côte Bleue to Cap Sicié. For our study, we focused on the Méjean site located 10 km west of Marseille (Fig. 1), where subsurface warming was generally strongest. We also took a broader view of the northwestern Mediterranean Sea in order to visualize the specificity of the Marseille region. To do this, we compared temperature trends at Méjean with those recorded at T-MEDNet points in Banyuls-sur-Mer and Villefranche-sur-Mer, located around 200 km to the southwest and northeast of Marseille (locations in Fig. 1). As mentioned in Sect. 2, Banyuls-sur-Mer on the western coast of the Gulf of Lion is subject to frequent downwellings, and Villefranche-sur-Mer on the Ligurian coast is strongly impacted by the Northern Current.

To link the intensity of the 2022 MHW with the extreme impacts on benthic communities down to depths of 30 m, we used a dataset compiled by scientists and marine-protected-area managers in 2022, after the MHW. This dataset is the largest available for monitoring a mass mortality event for benthic organisms in the Mediterranean Sea. The in situ data were acquired using the methods detailed by Estaque et al. (2023), who analyzed some of the data in detail for the Parc National des Calanques area. Here, the dataset consists of in situ data on the health of 18 465 colonies of red gorgonians (*P. clavata*), white gorgonians (*Eunicella singularis*), and yellow gorgonians (*Eunicella cavolini*) from 298 populations dwelling between the surface and 40 m depth. The data used allow us to compare the impact between the Parc National des Calanques (PnCal), the Parc Marin de la Côte Bleue (PMCB), the Cap Sicié (CS), and the Parc National de Port-Cros (PNPC) in relation to the differences in intensity of the 2022 MHW event.

4 Results

4.1 Assessment of the simulation and hydrological characteristics during summer 2022

Figure A1 in the Appendix shows the temporal evolution of measured and simulated temperature at Méjean between 5 and 40 m and between 2012 and 2022. The simulation shows a cold bias of around 0.5 °C at all levels, with uneven performance from year to year, particularly at 20 m depth, suggesting an uncertainty in the representation of the thermal gradient of the highly stratified layer beneath the surface mixed layer. The correlations between the observed and simulated series are above 0.95. Rapid temperature variations in summer, reflecting the succession of upwelling and stratification events, are visible at all levels and are well synchronized, indirectly indicating a correct representation of wind in the simulation. The maximum of the series at 5 m is 27.8 °C in terms of hourly values, reached in August 2022 (28.5 °C at Riou 20 km further south; see location in Fig. 1). The duration of exceedance of the 25 °C value in 2022 is also the longest of the decade. The simulation agrees with observations on these two extremes of temperature and duration.

Figure 2a–d zoom in on Fig. A1 from June to the end of September 2022. Correlations between observed and simulated series range from 0.88 at 40 m to 0.96 at 5 m. The model bias is greatest at 5 m (−1 °C) and varies between −0.18 and 0.15 °C at deeper levels. Warming episodes, highlighted in red, correspond to periods of continuous warming of at least 5 °C either at the surface or at 20 m. Northerly winds inducing cooling episodes are highlighted in blue when they reach 10 m s^{-1}.

Events above 25 °C at 5 m followed one another from 19 July to 9 September, with contrasting signatures further down. The event that peaked at the surface on 19 July resulted in an increase of around 3 °C at 20 m but was much less pronounced at greater depths. In contrast, the mid-August event was almost as warm at 20 m as at 5 m, with a signature at 30 m on 14 August, shortly after the surface maximum, of around +8 °C compared to at the beginning of the event. The temperature during the early September event

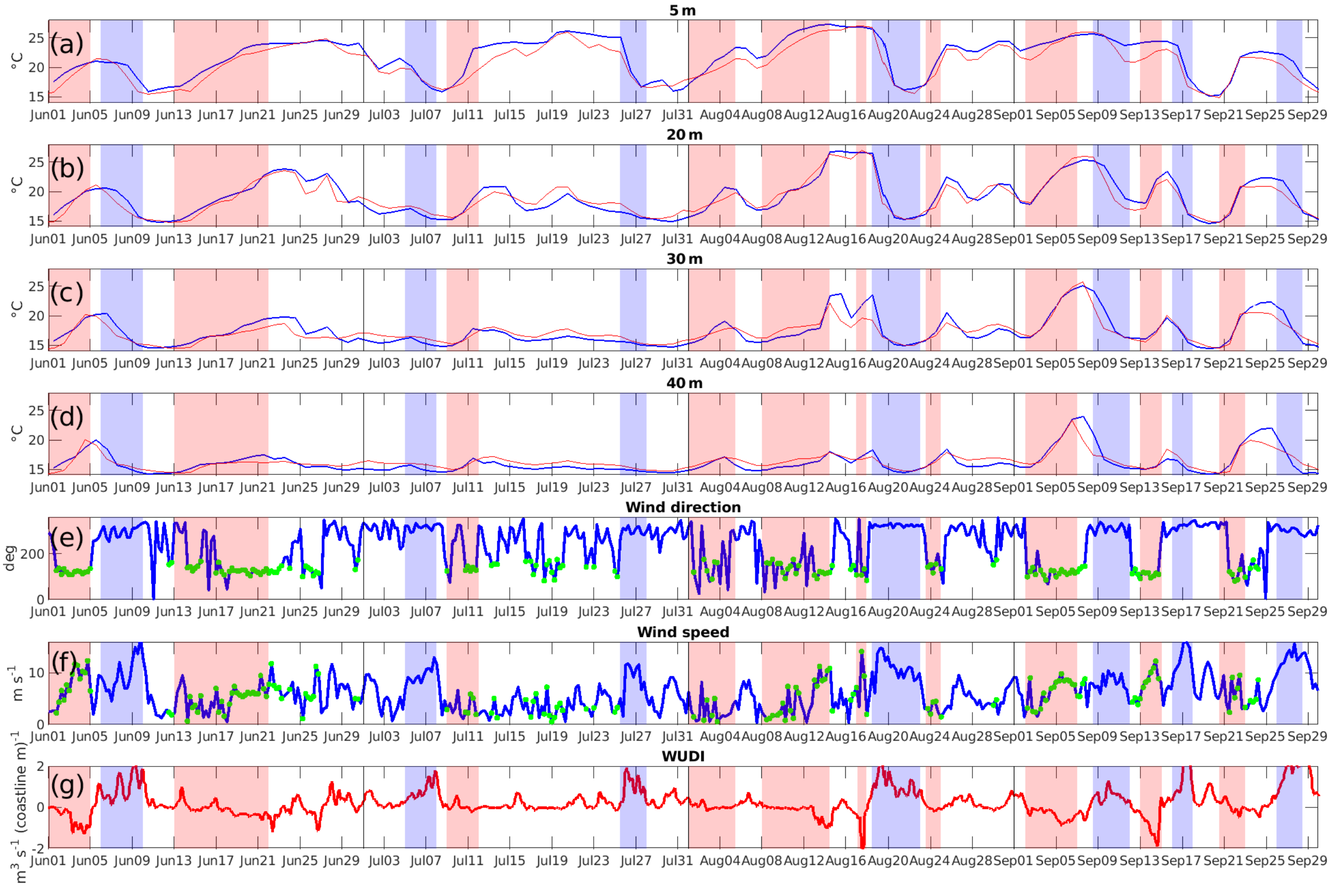

Figure 2. Observed (blue) and simulated (red) daily averaged temperature time series at the Méjean point of the T-MEDNet network during the summer of 2022 (June to September) from 5 to 40 m, as indicated above panels **(a)**–**(d)**. Wind direction and intensity (6 h moving average) near Marseille from the ECMWF model (ocean model forcing) are shown in **(e)** and **(f)**. The southeasterly winds are indicated in green. Wind-induced upwelling and downwelling index (6 h moving average) calculated at Méjean **(g)**. Warm events are highlighted by red stripes, and northerly winds associated with cooling are highlighted by blue stripes.

was almost uniform down to 30 m ($T > 25$ °C) and reached 24 °C at 40 m.

Figure 3 compares the local characteristics of the subsurface heatwave observed by the T-MEDNet network and simulated along the counterclockwise pathway of the Northern Current at Villefranche-sur-Mer, Méjean, and Banyuls-sur-Mer. In contrast to Méjean, Villefranche-sur-Mer's summer temperatures in 2022 did not vary greatly. The warm period extends over more than 2 months and generally involves a well-stratified surface layer. In Banyuls-sur-Mer, surface water temperatures are also more continuous than in Méjean but are significantly lower than in Villefranche. On the other hand, the heat is distributed over a much thicker layer, evoking the recurrent presence of downwellings. The simulation reproduces the thermal regime at the various sites with shortcomings such as the underestimation of the surface layer temperature at Villefranche-sur-Mer.

4.2 Meteorological characteristics during summer 2022

Figure 2e and f show the wind direction and intensity of the ECMWF model near Marseille. For greater visual clarity, hourly winds are averaged over 6 h. Figure 2g illustrates the wind-induced upwelling and downwelling index (WUDI), as outlined by Odic et al. (2022), calculated with the ECMWF model at the Méjean probe location. This index quantifies the horizontal Ekman transport within the model, exhibiting a positive or negative value, indicative of upwelling or downwelling, respectively. In line with climatology, the strongest winds blow from the mainland. Whenever the north–northwestern wind exceeds 10 m s^{-1}, a surface temperature drop of at least 5 °C is observed and simulated over the following days. This is the case for events starting on 6 June; 5 and 26 July; 18 August; and 9, 16, and 26 September. These upwellings are also visible below the surface (especially if warming has taken place beforehand, as in the cases of 6 June and 9 September). In this respect, it is worth noting that temperatures drop at depth around 24 h before

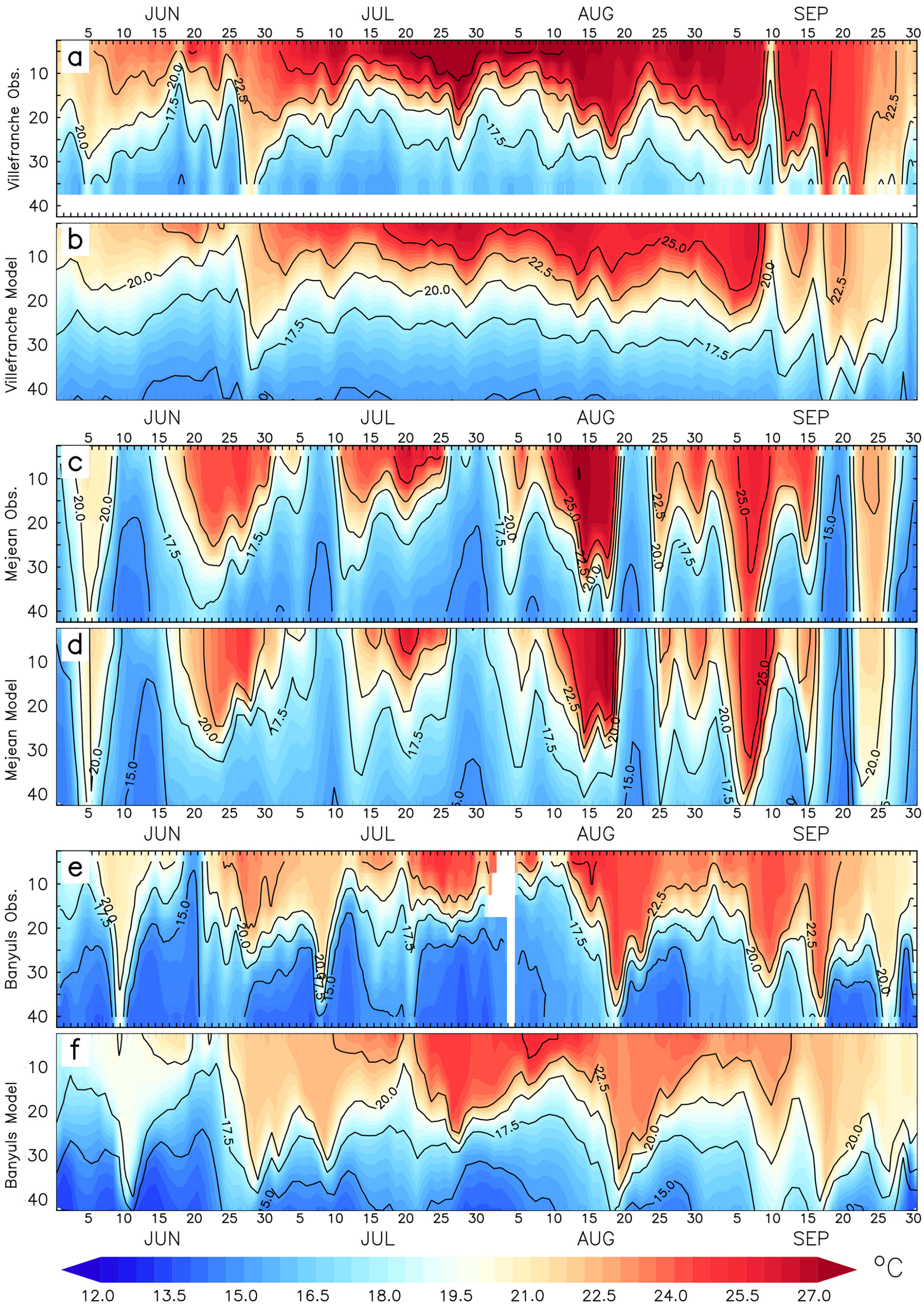

Figure 3. Hovmöller diagrams of the temperature (°C) profiles (m) given by the T-MEDNet probes **(a, c, e)** and the model **(b, d, f)** at the locations of Villefranche-sur-Mer **(a, b)**, Méjean **(c, d)**, and Banyuls-sur-Mer **(e, f)** (see locations in Fig. 1). Isotherms every 2.5 °C. The probe diagrams are smoothed vertically and over 24 h in order to facilitate optimal viewing.

they do so at the surface (see, for example, the 6 June event). In all of the aforementioned instances, the WUDI is greater than $+0.5\,\mathrm{m^3\,s^{-1}}$ per coastline meter, which is consistent with the previous identifications of upwelling.

During summer 2022, warm events are characterized by lower wind intensities than northerly wind events. They are classified here as either weak winds (typically below $5\,\mathrm{m\,s^{-1}}$) or moderate southeasterly winds (typically above $5\,\mathrm{m\,s^{-1}}$ and rarely above $10\,\mathrm{m\,s^{-1}}$). All cases of weak or moderate southeasterly winds are indicated in green in Fig. 2e and f and are all located in warm periods. Specifically, the periods in question are 1–5, 13–22 June, 9–12 July, 1–4, 8–14, 23–25 August, and 2–7 and 13–15 September. For moderate wind speeds, the negative WUDI index below $-0.5\,\mathrm{m^3\,s^{-1}}$ per coastline meter suggests a potential contribution of downwellings to warming episodes.

In order to characterize southeasterly winds over the summer of 2022 in relation to climatology, statistics have been compiled over the period 2012–2022. Each month, the time integral of the negative WUDI (i.e., downwelling index) is calculated. Figure A2 shows the climatology of this index, the dispersion over 11 years, and the value for 2022. Summer – and, especially, July and August – shows very low values compared with autumn and winter, which also show very high interannual variability. For the summer of 2022, downwelling dynamics are particularly weak in July, while, in August, they are the strongest in the series while remaining low compared to the rest of the year.

Figure 4 shows the surface wind fields during the two warmest events at depth (30 m) on 13–14 August and 5–7 September. In both cases, a low-pressure area was present over western Europe (western France in the first case and the British Isles in the second case), leading to a southerly flow over the Mediterranean Sea, which penetrated the mainland in the Gulf of Lion. This flow in the lower layers of the atmosphere was strongly influenced and accelerated by the relief, especially in Corsica and Sardinia, bypassed by veins of wind between and around the two islands. These wind veins converged in the eastern Gulf of Lion, influenced by the topography of the Provençal coast and the edge of the Alpine chain, producing a noticeable acceleration in the vicinity of Marseille.

4.3 Marine heatwaves

The warmest event at the surface and at 20 m at Méjean occurred in mid-August. At 30 and 40 m, temperatures peaked later in the season, during the 6 September event. Events were longest at the surface: the major event in mid-August lasted around 2 weeks. While warm events were characterized by weak wind or moderate southeasterly wind conditions, they were stopped by northerly wind gusts along the northern coast (Fig. 2). The points discussed in the following three subsections are as follows: warming during weak wind conditions (Sect. 4.3.1) and during moderate southeasterly winds (Sect. 4.3.2) and the sensitivity of subsurface warming to the duration of southeasterly winds (Sect. 4.3.3).

4.3.1 Case of weak winds: impact of pre-existing upwelling

The upwellings that characterize the region studied here are mechanisms that a priori protect the coast from MHWs by renewing surface water with deep cold water. However, Barrier et al. (2016) have highlighted a collateral effect that occurs when the upwelling stops in the form of intrusions of the Northern Current onto the Gulf of Lion shelf, with a delay of 1 d after the wind relaxation. The impact of these intrusions on the occurrence of heatwaves in the eastern Gulf of Lion is described in this section.

Five warming episodes were considered, namely those of 13–18 June, 9–12 July, 1–4, and 8–12 and 23–25 August, characterized by winds of less than $5\,\mathrm{m\,s^{-1}}$, mostly blowing from the southeast, with occasional short spells from the northwest (Fig. 2). For each of these events, the temperature rise at 5 m ranged from 4 to 7 °C (on average, 5.4 °C). At 20 m, the warming was slightly lower (5 °C on average). It continued to decrease at 30 m (3 °C on average) and at 40 m (1.9 °C on average) (more details on the different events in Table A1). The warming at 5 m cannot be due to a downwelling as this would imply a considerable temperature gradient between the surface and 5 m. Let us now consider the role of the solar radiation to explain this warming. For the 9–12 July event, over 2 d, the warming at 5 m was 6.7 °C, and that at 20 m was 5.4 °C. The warming induced by the absorption of the heat associated with solar radiation, equal to $320\,\mathrm{W\,m^{-2}}$ on average over 24 h, is around 0.8 °C. Warming is therefore almost caused by an ocean-internal mechanism internal. For each event considered, the warming at Méjean started between 1 and 3 d after the end of a northerly gale (varying in intensity from 8 to $15\,\mathrm{m\,s^{-1}}$) and at the end of the associated upwelling, which fits perfectly with the observations of Barrier et al. (2016) cited above. This process is responsible for the observed warming, and it implies that the water mass advected during the Northern Current intrusion was much warmer than that present on the Gulf of Lion prior to the upwelling. The eastern part of the Gulf of Lion is particularly favorable for this situation as it borders to the east of 6° E, an area much less exposed to northerly winds and therefore much more continuously warm at the surface (see the time series at Villefranche-sur-Mer in Fig. 3a).

As an example, Fig. 5a–c show the surface temperature and current for the second warming episode on 8, 12, and 15 July: at the peak of the northerly wind and upwelling on 8 July and during and at the end of the warming phase on 12 and 15 July, respectively. The intrusion of a branch of the Northern Current advecting warm water is visible along the coast in the Marseille area after the stop of the northerly wind: the warm-water mass was located east of 6° E on 8 July (Fig. 5a) and then 50 km further west on 12 July (Fig. 5b)

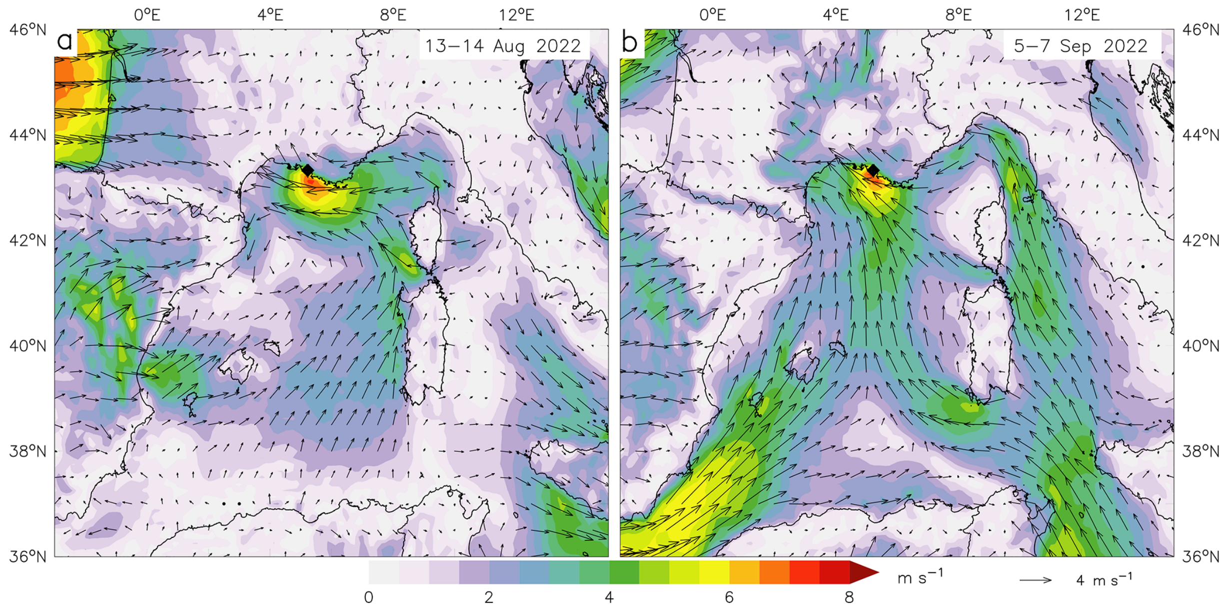

Figure 4. ECMWF wind field ($m\,s^{-1}$) at 10 m averaged over the two warmest subsurface periods: **(a)** 13–14 August 2022 and **(b)** 5–7 September 2022. The black diamond represents the Méjean observation point.

and around 100 km (up to 5° E) on 15 July (Fig. 5c). It is also interesting to note that the strong, sustained northerly wind ($\sim 10\,m\,s^{-1}$ for 4 d) which preceded the warming episode produced marked hydrological structures (Fig. 5a) such as the upwelling front stretching southward off Marseille and, further west, organized cross-shore currents. These structures, which persist for a few days, probably hinder the westward progress of warm waters.

4.3.2 Case of moderate to strong southeasterly winds

Odic et al. (2022) showed the tight correlations between downwelling-favorable winds and 35 m temperature anomalies along the northwestern Mediterranean shorelines. They quantified that the 75th percentile of the WUDI index for downwelling corresponded to an alongshore wind close to $5\,m\,s^{-1}$ and a temperature response of +3 °C at 35 m for stratified conditions. Here, we examine the impact of such downwelling on subsurface heatwaves. According to Juza et al. (2022) and Darmaraki et al. (2024), such downwelling processes may indeed facilitate the vertical extension of heatwaves in the western Aegean and in northeastern Crete.

Here, we consider the two cases associated with the warmest temperatures at 20 m: the 12 to 14 August event extended by a secondary peak on the 17th and the 2 to 7 September event. In both cases, the southeasterly wind presented in Fig. 4 exceeded $8\,m\,s^{-1}$, and the WUDI index fell, showing coastward transports of over $0.5\,m^3\,s^{-1}$ per coastline meter that lasted 2 d (Fig. 2). The vertical distribution of warming was quite different from that of low winds (Figs. 2 and 3, Table A1): warming was minimal at the surface as temperatures were already high at the start of both events and increased down to 30 m, with values of 5.5 °C in August and 8.8 °C in September (compared with 2–3.6 °C for weak winds). At 40 m, warming was 2 °C for the first (and shorter) event and 8.5 °C for the second one. Again, in contrast to the low-wind cases, the northerly wind preceding the 6 September event was weak (less than $10\,m\,s^{-1}$) and of short duration (from 31 August to 1 September), and, as a result, the associated upwelling (Fig. 5d) and the currents on the inner shelf were poorly developed, and the intrusion of the Northern Current associated with the cessation of upwelling was weak. The warming during this event was therefore rather related to the southeasterly wind causing surface water to pile up against the coast, inducing the downwelling of warm surface water and, finally, through geostrophy, the development of an alongshore westward jet. The persistence of the easterly wind (6 d without interruption) and the weak currents that prevailed before favored the establishment of this alongshore circulation at the whole continental shelf scale, warming a large part of the coastal zone of the Gulf of Lion between 1 and 6 September, as shown in Fig. 5f. At a depth of 30 m, Fig. 6a–c show the pre-event and peak temperatures and their differences, indicating that the eastern Gulf of Lion was warmed up by around 7 °C over 600 km^2 from 5.62° E of Cassis to 4.85° E near the Rhône mouth. Further west, the coastal strip extending up to the 60 m isobath was heated by 2 to 4 °C. The similarity between the area of maximum warming and that of maximum downwelling-favorable winds (Fig. 4b) is remarkable.

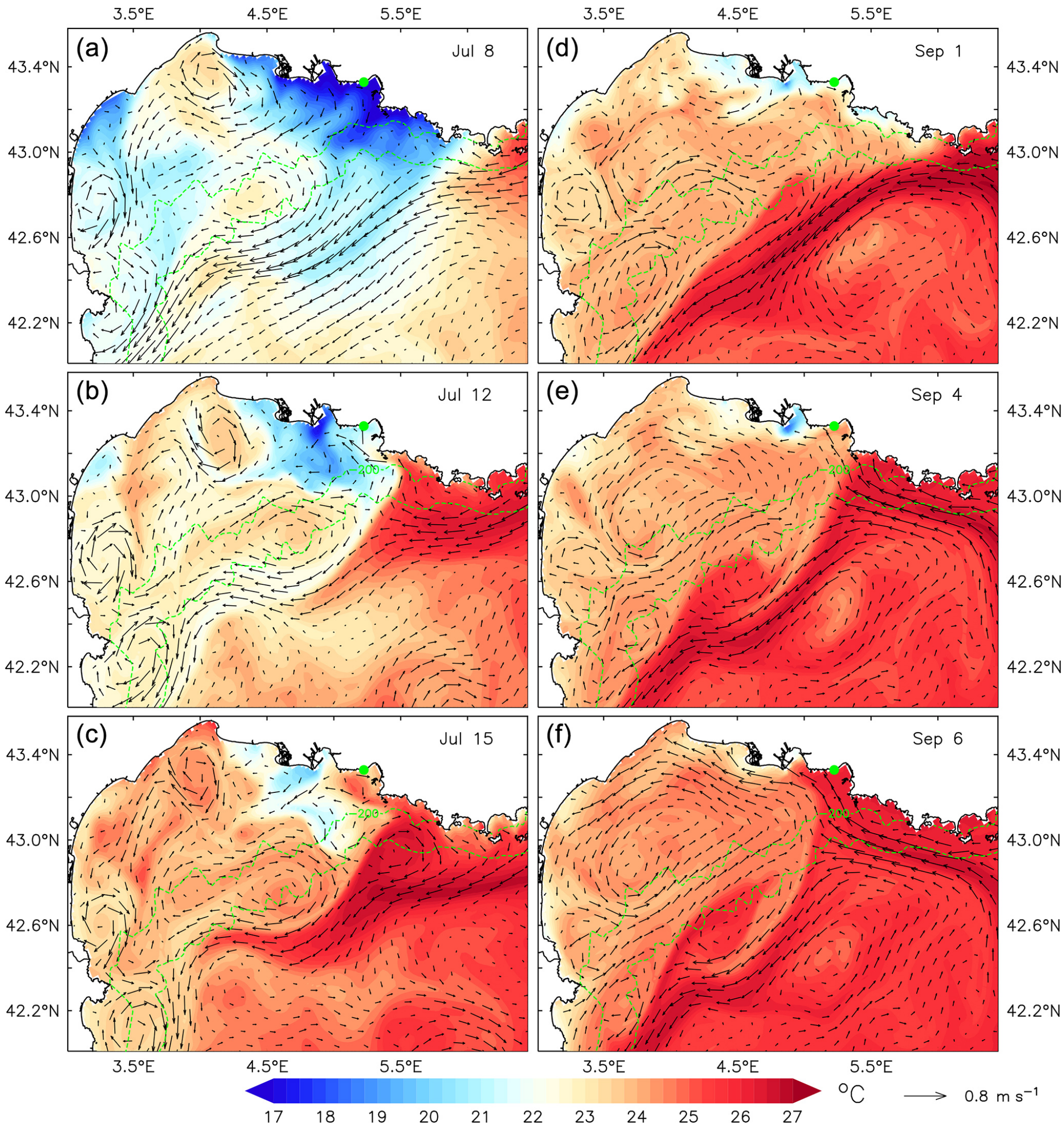

Figure 5. Surface temperature (°C) and current simulated for the surface warming event of July **(a–c)**: **(a)** 8 July (during the upwelling), **(b)** 12 July (the day after the wind stopped), and **(c)** 15 July. Same for the subsurface warming event of September **(d–f)**: **(d)** 1 September, **(e)** 4 September, and **(f)** 6 September. The green point represents the Méjean T-MEDNet observation point. The dashed green lines are the 200 and 1000 m isobaths.

4.3.3 Sensitivity of heat penetration at depth to the duration of the southeasterly wind

We consider the mid-August event at Méjean, the warmest event of the summer at the surface. We described it as a succession of two main events (Fig. 2e and f) – one with weak winds from 8 to 12 August and a second one with sustained southeasterly winds from 12 to 14 August (Fig. 4a) – when sponge mortality in the Bay of Marseille began to be observed. This mortality was massively concentrated in the 0–25 m layer and more sparsely at 30 m. The second event is not detailed because it is similar to the one in September, except that, as mentioned in the previous paragraph, the duration of the southeasterly wind was shorter, and the deep warming was lower in August. To understand the relation between warming and the duration of the southeasterly wind, we conducted a study of the sensitivity to this duration. The sustained wind event lasted about 40 h. As the occurrence of southeasterly winds is high in August 2022 (Fig. A2), we limit the extension of the southeasterly wind period by 1 d. This modification was made during the weakening wind period from 13:00 UTC on 14 August to 13:00 UTC on 15 August, where we substituted the stronger wind from the period of 01:00 UTC on 13 August to 01:00 UTC on 14 August. Due to the fact that the temperature at 30 m of the reference simulation is underestimated from 15 to 18 August by 3 °C on

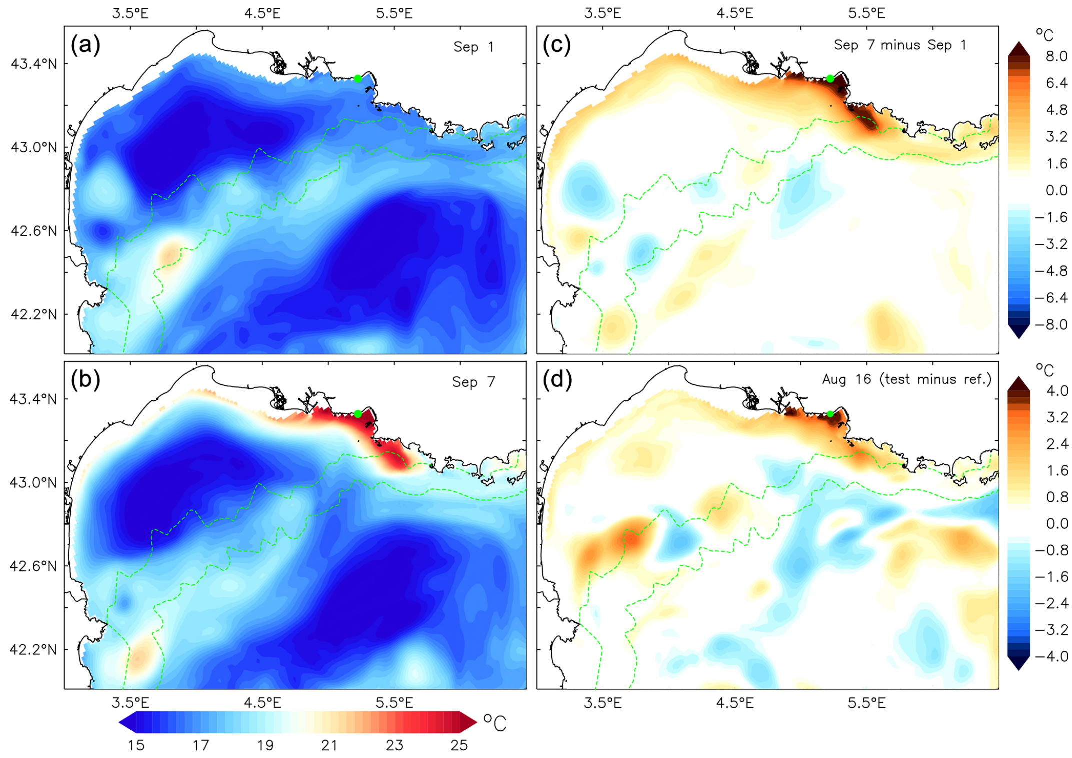

Figure 6. (a–c) September event. Temperature (°C) at 30 m depth before the September subsurface warming event (**a**: 1 September) and at the peak of the event (**b**: 7 September). **(c)** Warming between these two dates. **(d)** August event. Temperature difference (°C) at 30 m depth on 16 August between the test (extension of the southeasterly wind period) and the reference simulations. The dashed green lines are the 200 and 1000 m isobaths.

average (Fig. 2), we will subsequently present differences between the test and the reference simulations rather than the biased warming for each simulation. Figure 6d represents this temperature difference at 30 m on 16 August. As expected, the lengthening of the period of southeasterly winds results in increased warming. The temperature difference at 30 m from 15 to 17 August exceeds 3.5 °C around Marseille. The daily average temperature observed on 14 and 15 August was 23.8 °C. If we transpose the results of the sensitivity test to the observed series, we deduce that the temperature at 30 m would have reached the value at 20 m. This would likely have led to a deepening of the mass mortality zone to 30 m instead of 25 m and partial mortality at 35 m due to an increased warming of 1.3 °C compared to the reference simulation. It can be seen that the maximum warming along the Gulf of Lion coast is in the same place as in the early September situation (Fig. 6c). This is also where the southeasterly wind is strongest during the warming period (Fig. 4a).

4.4 Impact on marine benthic communities

Under the influence of southeasterly wind regimes, which induced warm-water downwelling to a depth of 30 m, and MHWs that exhibited heightened intensity across a 600 km^2 area between 5.62° E (east of Cassis) and 4.85° E (near the Rhône River mouth), gorgonian mortality was observed to be more severe and extended to greater depths within this region. Generally speaking, the impact on gorgonian populations appears to be most severe in the Cap Sicié, Parc National des Calanques, and Parc Marin de la Côte Bleue areas, particularly for the red gorgonian (*P. clavata*). For this species, which is the most sensitive, more than 50 % of the populations monitored in the 20 to 30 m depth range in the PnCal showed a severe impact (> 60 % of affected colonies) compared with less than 10 % in Port-Cros for the same depth range (Fig. 7). More specifically, in line with the MHWs observed, no impact has been recorded for the *E. cavolini* in the PNPC area, while a sometimes severe impact has been recorded for this species in the PnCal and PMCB areas. The same observation was made for *E. singularis*, whose populations were less affected (10 %–30 % affected colonies) in the PNPC area for the 10–20 m depth range and were not affected at deeper levels, while the populations were sometimes severely affected (> 60 % of affected colonies) down to 20 m in the PnCal area and moderately affected (30 %–60 % of affected colonies) in the PMCB area down to 30 m. These observations suggest a greater impact at greater depths (down to 30 m) for the gorgonian populations around the Marseille region than within the PNPC.

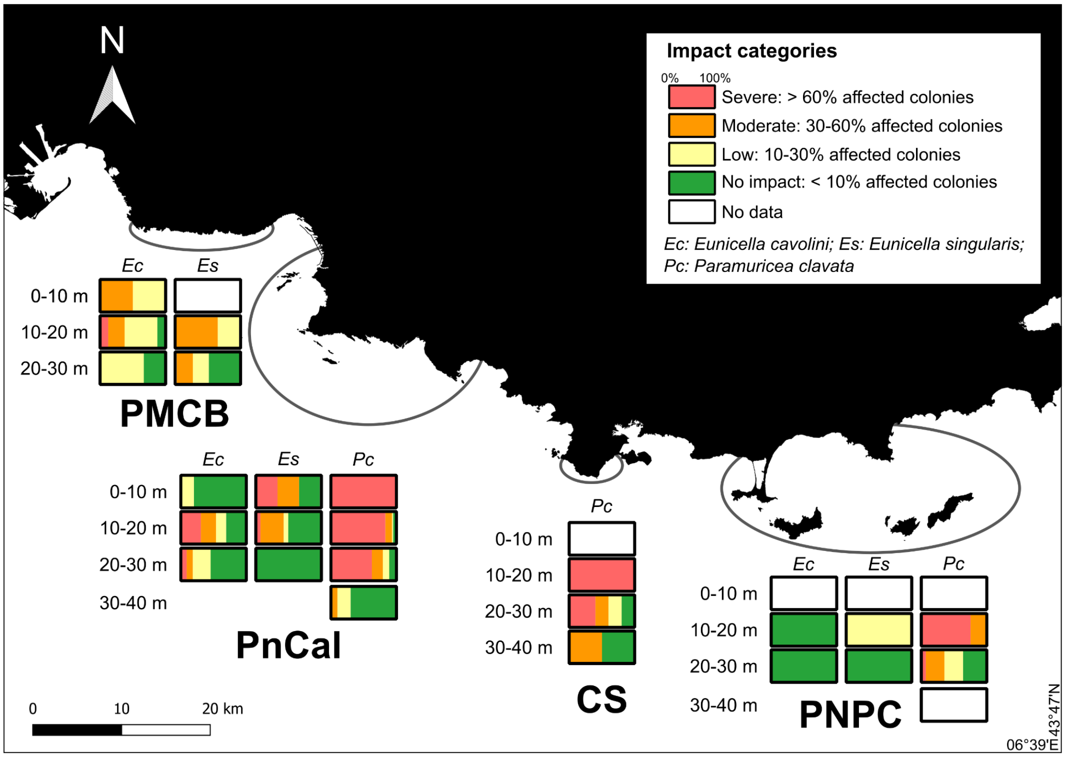

Figure 7. Map showing the severity of the impact of the mass mortality event on the gorgonian populations of the Parc Marin de la Côte Bleue (PMCB), the Parc National des Calanques (PnCal), the Cap Sicié (CS), and the Parc National de Port-Cros (PNPC). The impact on populations is represented by 10 m depth ranges between the surface and 40 m. See Estaque et al. (2023) for more details on the monitoring method. Data for *P. clavata* in the PnCal are presented in more detail in Estaque et al. (2023).

4.5 Variability of deep heatwaves on a regional scale

Figure 3 illustrates the major spatial variability of the upper-layer temperature chronology on a regional scale. The upwelling and downwelling temperature alternations discussed for Méjean are much reduced at the other two sites. Villefranche-sur-Mer is characterized by the presence of warm water throughout the summer in the surface layer due to warming as a result of the Northern Current flowing close to the coast and weak winds. Surface temperatures are frequently as high as the maximum recorded at Méjean on 15 August. The two deep heatwave events studied at Méjean are also present at Villefranche-sur-Mer, also indicating the influence of the easterly wind in this region, albeit this is attenuated compared with the Marseille area (Fig. 3), reducing the depth impacted by downwelling by about 10 m. At Banyuls-sur-Mer, the situation is different from that at the two other sites, with repeated temperature peaks almost reaching 40 m. The deep heatwave events of mid-August and early September studied at Méjean are also present, albeit a few days late, but temperature peaks are lower than at the two other sites, reflecting the reduced influence of the Northern Current over most of the Gulf of Lion shelf and the frequent presence of dry northerly winds cooling the surface.

5 Discussion and perspectives

During the summer of 2022, the atmospheric heatwaves that hit western Europe gave rise to extreme marine heatwaves across the western Mediterranean, as shown by Guinaldo et al. (2023). Despite being a coastal zone relatively tempered by the recurrence of northerly winds and associated upwelling, the east of the Gulf of Lion and the very rich benthic ecosystems that it shelters have been exposed to short periods of exceptional temperatures.

The succession of hot and cold events in summer 2022 has been successfully reproduced by a numerical simulation: all of the events have been simulated, and the correlations are generally above 0.9. To go further, the precise reproduction of warm events is a major issue when it comes to determining the crossing of thermal thresholds representing the survival of marine species. In order to improve this precision, we identify two sensitive points here. On the one hand, a higher resolution of the horizontal grid will improve the description of the strong bathymetric gradients characteristic of the coastal area around Marseille and further east, along the Ligurian coast, and, consequently, the representation of horizontal and vertical movements. On the other hand, the accuracy of the near-shore wind field is likely to be crucial for the accuracy of simulated temperatures due to the influence of topography on wind channeling and acceleration. Exploring the uncertainties of these two origins would be informative in improving the description of risk areas and in predicting extreme temperatures with better precision without unnecessarily increasing computational costs.

Despite the uncertainties, our modeling results provide insights into the two types of heatwaves that were recorded in 2022. The first type of heatwave is a surface phenomenon. The physical processes at play are recurrent when the northerly winds and induced upwelling stop and when the wind speed following the northerly wind is less than $\sim 5\,\mathrm{m\,s^{-1}}$. This succession of meteorological conditions causes an intrusion of warm water from the Northern Current along the northeastern coast of the Gulf of Lion. In these situations, only the 5 m level exceeded 25 °C. In summary, these events renew the coastal water mass by an advection of warm water until the following northerly gale which replaces the surface water with cold subsurface water. The second type of heatwave, more dramatic because it affected depths of 30 to 40 m, is generated by southeasterly winds (around $8–10\,\mathrm{m\,s^{-1}}$). Surface heating is still due to the advection of warm water from the east, but it is pushed downward by wind-induced coastal downwelling. The strength and duration of the southeasterly wind are crucial parameters which determine the depth impacted. This second type of event, marked by pronounced subsurface heatwaves induced by downwelling, was highlighted by Juza et al. (2022) and Darmaraki et al. (2024) in other Mediterranean regions.

On a regional scale (~ 200 km), we have shown considerable variability in surface and deep heatwaves for two reasons: (i) the channeling of northerly and easterly winds by the continental relief associated with the complex shape of the coastline, which produces localized upwelling and downwelling, and (ii) warming by the Northern Current, whose influence is great along the Ligurian coast and reduced in the western part of the Gulf of Lion. This high spatiotemporal variability in heatwaves in coastal areas contrasts with that of heatwaves in open seas, which are much more widespread and also more spatially homogeneous. The T-MEDNet network is an extremely valuable tool for documenting this variability and providing a database for validating high-resolution numerical models.

The severity of the 2022 summer in relation to benthic species is the result of the superposition of two conditions, both exceptional, namely (1) the atmospheric heatwave which led to an exceptional warming of the surface of the western Mediterranean Sea and (2) the two southeasterly wind events in mid-August and early September which caused these warm waters to plunge to depth. These latter events are rare in summer, as evidenced by the monthly downwelling index, which is the highest in the decade for August and to which the major event that occurs at the beginning of September must be added. The occurrence of sustained southeasterly winds in summer, when surface temperatures are warmest, therefore constitutes a major danger for coastal ecosystems, particularly for benthic species located above 40 m depth. The coastal region around 30 km on either side of Marseille, with its remarkable habitats, is at far greater risk than the rest of the Gulf of Lion due to the acceleration of southeasterly winds caused by the topography, which locally intensifies downwelling. Indeed, we have verified that the acceleration shown here for the two major events of August and September 2022 exists in most of the southeasterly wind situations occurring between June and September over the period 2012–2022. This is indirectly confirmed by Odic et al. (2022), who, using the wind from the ERA5 reanalysis to calculate upwelling and downwelling indices, showed that the Marseille vicinity is not only the most powerful upwelling zone in the northern Gulf of Lion but also the most exposed to downwelling.

Global warming was proven to have contributed to the extreme temperatures experienced in the western Mediterranean Sea during the summer of 2022 (Faranda et al., 2023). Exploring the coincidence of southeasterly winds and surface heatwaves in future climate scenarios would help anticipate the recurrence of massive mortality events and, ultimately, the disappearance of benthic populations, which are emblematic of the Calanques region of Marseille and of the Côte Bleue. Given the ongoing global warming trends, an increase in the frequency and intensity of MHWs in the affected depth zones (0–30 m) and deeper is expected. These extreme thermal events are likely to severely impact the potential recovery of benthic organism populations, and the potential role of refuge from deeper populations is not certain (Bramanti et al., 2023). Certain benthic species, such as gorgonians, play a crucial role as ecosystem engineers, contributing significantly to habitat complexity (Verdura et al., 2019). The collapse of these species would therefore lead to a marked reduction in structural diversity, with cascading effects on the broader ecosystem, including the disruption of ecological functions (Ponti et al., 2014) and the loss of vital ecosystem services (Estaque et al., 2023; Garrabou et al., 2021; Gómez-Gras et al., 2021). To mitigate these impacts, it is imperative to adopt multidisciplinary approaches that integrate ecological, oceanographic, and climatological data to better predict the occurrence and intensity of MHWs. Such strategies are essential for developing adaptive coastal area management and conservation efforts, with the goal of preserving the integrity of Mediterranean benthic communities and maintaining the ecosystem services they provide. In a context where management plans are predominantly designed within a two-dimensional framework (Jacquemont et al., 2024), this approach marks a critical advancement toward recognizing the ocean as a three-dimensional environment, particularly when establishing marine protected areas and conservation zones.

Finally, heatwaves will not only intensify in terms of frequency and intensity with climate change, but thermal stress will combine with other stresses whether it is linked to the long-term increase in anthropogenic CO_2 or to the short-term impact of heatwaves on the chemical and biogeochemical composition of water. An extension of this study toward the impact of the 2022 heatwaves on oxygen, pH, and chlorophyll concentrations in the Gulf of Lion is planned.

Appendix A

Table A1. Identification of the different surface and subsurface warm events. Warming (in °C) observed at Méjean over each period at different depths (T-MEDNet data).

	5 m warming	20 m warming	30 m warming	40 m warming
Surface event				
13–18 June	4.8	4.2	2.3	1.8
9–12 July	6.7	5.4	2.6	1.4
1–4 August	4.1	4.7	3.6	2.0
8–12 August	4.7	4.2	2.0	1.1
23–25 August	6.8	6.4	4.8	3.0
Average	*5.4*	*5.0*	*3.0*	*1.9*
Subsurface event				
12–14 August	0.6	5.6	5.8	1.9
2–7 September	2.1	7.5	8.8	8.5
Average	*1.4*	*6.5*	*7.3*	*5.2*

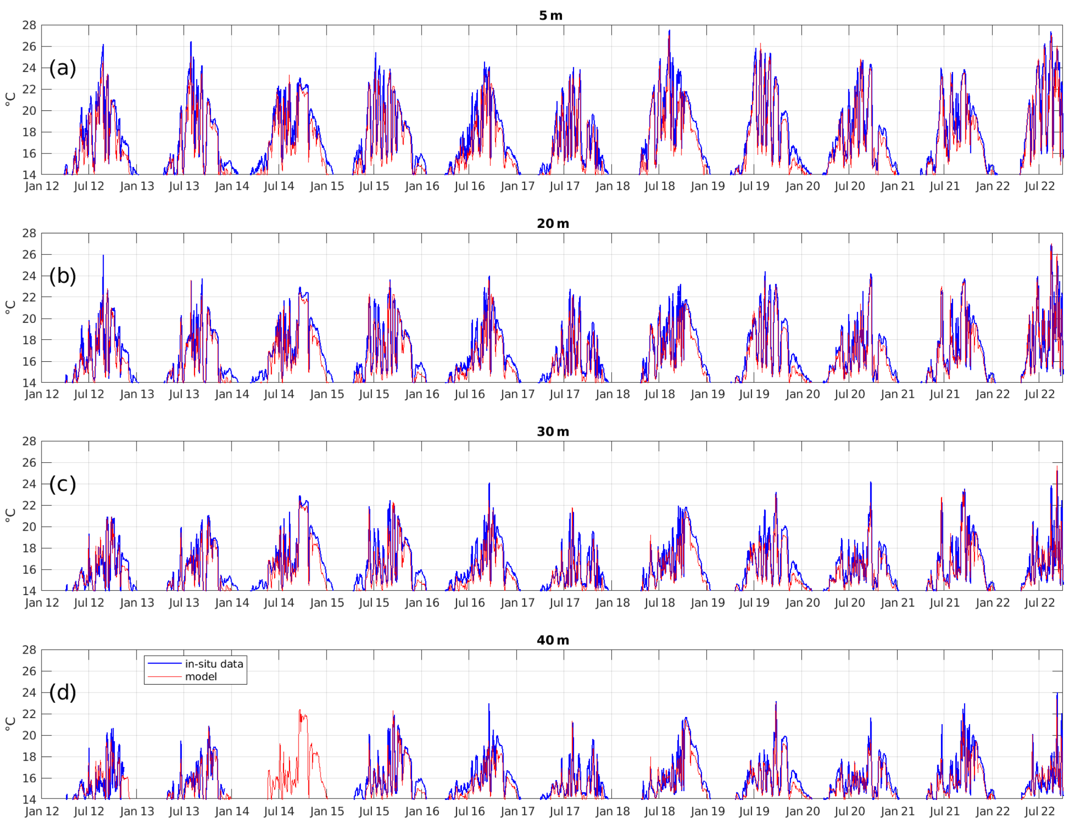

Figure A1. Observed (blue) and simulated (red) temperature time series at the Méjean station of the T-MEDNet network for 2012 to 2022 from 5 to 40 m, as indicated above the figures. The frequency shown is daily. Note the absence of in situ data in 2014 at 40 m due to technical problems.

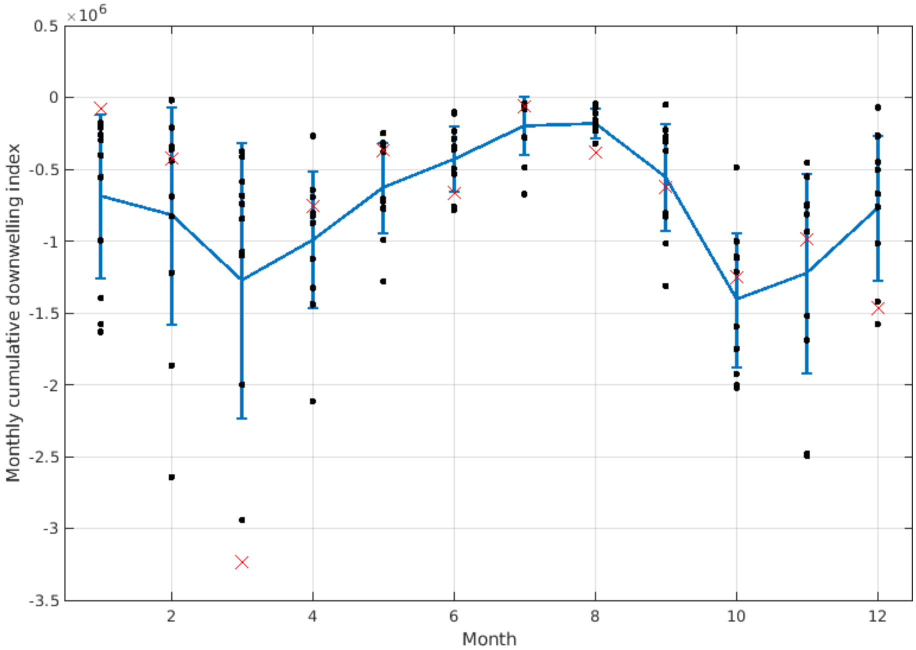

Figure A2. Monthly cumulative downwelling index (m^3 per coastline meter) off Marseille. Blue curve: climatology ± standard deviation calculated over 2012–2022. Black dots represent the monthly values for each year, and the red cross is for 2022.

Code availability. The source code of the model has been archived at https://doi.org/10.5281/zenodo.13774746 (Marsaleix, 2024).

Data availability. The T-MEDNet temperature data are available from https://t-mednet.org/ (T-MedNet, 2025).

Author contributions. CU and CE planned the study and conceptualized the paper. TE analyzed the biological data. The model was developed by PM. CE and PM performed the simulations. QBB analyzed the meteorological forcing. CE and TE wrote the first version of the paper. All of the co-authors edited and corrected the text.

Competing interests. The contact author has declared that none of the authors has any competing interests.

Disclaimer. Publisher's note: Copernicus Publications remains neutral with regard to jurisdictional claims made in the text, published maps, institutional affiliations, or any other geographical representation in this paper. While Copernicus Publications makes every effort to include appropriate place names, the final responsibility lies with the authors.

Special issue statement. This article is part of the special issue "Special issue on ocean extremes (55th International Liège Colloquium)". It is not associated with a conference.

Acknowledgements. The in situ temperature data have been provided by the regional temperature observation network T-MEDNet (https://t-mednet.org/; last access: 16 July 2025) for the site Méjean (Dorian Guillemain, OSU Institut Pythéas), for the site Villefranche-sur-Mer (Nuria Teixido and Steeve Comeau, Laboratoire d'Océanographie de Villefranche-sur-Mer), and for the site Banyuls-sur-Mer (Ronan Rivoal, Réserve Naturelle Marine de Cerbère Banyuls/Conseil Départemental des Pyrénées Orientales). For the health data on gorgonian populations, we would like to thank Eric Charbonnel, Patrick Bonhomme, Pauline Vouriot, Stéphane Sartoretto, Quentin Schull, Bastien Mérigot, and the entire Septentrion Environnement team. The SYMPHONIE model and the simulations produced are distributed by the national service SIROCCO (https://sirocco.obs-mip.fr, last access: 16 July 2025) of CNRS-INSU, coordinated by the ILICO research infrastructure. The simulations were performed using high-performance-computing (HPC) resources from CALMIP (grant no. P09115) and from GENCI-CINES (grant no. AD010110088R2). Claude Estournel is grateful to Pierre Chevaldonné and Thierry Perez for their constructive feedback.

Financial support. This study was funded by the OFB (Office français de la biodiversité) and ILICO littoral and coastal research infrastructure (https://www.ir-ilico.fr/?PagePrincipale) through the INTEGRATION workshop for the study of marine heatwaves along the French coastline. It was also supported by the PPR-RiOMar project, a French government grant managed by the Agence Nationale de la Recherche under the France 2030 program (grant no. ANR 22 POCE 0006).

Review statement. This paper was edited by Matjaz Licer and reviewed by Francisco Pastor and one anonymous referee.

References

Barrier, N., Petrenko, A. A., and Ourmières, Y.: Strong intrusions of the Northern Mediterranean Current on the eastern Gulf of Lion: insights from in-situ observations and high resolution numerical modelling, Ocean Dynam., 66, 313–327, https://doi.org/10.1007/s10236-016-0921-7, 2016.

Bensoussan, N., Romano, J. C., Harmelin, J. G., and Garrabou, J.: High resolution characterization of Northwest Mediterranean coastal waters thermal regimes: To better understand responses of benthic communities to climate change, Estuar. Coast. Shelf Sci., 87, 431–441, https://doi.org/10.1016/j.ecss.2010.01.008, 2010.

Bramanti, L., Manea, E., Giordano, B., Estaque, T., Bianchimani, O., Richaume, J., Mérigot, B., Schull, Q., Sartoretto, S., Garrabou, J. G., and Guizien, K.: The deep vault: a temporary refuge for temperate gorgonian forests facing marine heat waves, Mediterran. Mar. Sci., 24, 601–609, https://doi.org/10.12681/mms.35564, 2023.

Crisci, C., Bensoussan, N., Romano, J.-C., and Garrabou, J.: Temperature anomalies and mortality events in marine communities: Insights on factors behind differential mortality impacts in the NW Mediterranean. PLoS One, 6, e23814, https://doi.org/10.1371/journal.pone.0023814, 2011.

Damien, P., Bosse, A., Testor, P., Marsaleix, P., and Estournel, C.: Modeling post-convective submesoscale coherent vortices in the northwestern Mediterranean Sea, J. Geophys. Res.-Oceans, 122, 9937–9961, https://doi.org/10.1002/2016JC012114, 2017.

Darmaraki, S., Denaxa, D., Theodorou, I., Livanou, E., Rigatou, D., Raitsos E. D., Stavrakidis-Zachou, O., Dimarchopoulou D., Bonino, G., McAdam, R., Organelli, E., Pitsouni, A., and Parasyris, A.: Marine Heatwaves in the Mediterranean Sea: A Literature Review, Mediterran. Mar. Sci., 25, 586–620, https://doi.org/10.12681/mms.38392, 2024.

Drobinski, P., Ducrocq, V., Alpert, P., Anagnostou, E., Béranger, K., Borga, M., Braud, I., Chanzy, A., Davolio, S., Delrieu, G., Estournel, C., Filali Boubrahmi, N., Font, J., Grubišić, V., Gualdi, S., Homar, V., Ivančan-Picek, B., Kottmeier, C., Kotroni, V., Lagouvardos, K., Lionello, P., Llasat, M. C., Ludwig, W., Lutoff, C., Mariotti, A., Richard, E., Romero, R., Rotunno, R., Roussot, O., Ruin, I., Somot, S., Taupier-Letage, I., Tintore, J., Uijlenhoet, R., and Wernli, H.: HyMeX: A 10-Year Multidisciplinary Program on the Mediterranean Water Cycle, B. Am. Meteorol. Soc., 95, 1063–1082, https://doi.org/10.1175/BAMS-D-12-00242.1, 2014.

Ducrocq, V., Braud, I., Davolio, S., Ferretti, R., Flamant, C., Jansa, A., Kalthoff, N., Richard, E., Taupier-Letage, I., Ayral, P., Belamari, S., Berne, A., Borga, M., Boudevillain, B., Bock, O., Boichard, J., Bouin, M., Bousquet, O., Bouvier, C., Chiggiato, J., Cimini, D., Corsmeier, U., Coppola, L., Cocquerez, P., Defer, E., Delanoë, J., Di Girolamo, P., Doerenbecher, A., Drobinski, P., Dufournet, Y., Fourrié, N., Gourley, J. J., Labatut, L., Lambert, D., Le Coz, J., Marzano, F. S., Molinié, G., Montani, A., Nord, G., Nuret, M., Ramage, K., Rison, W., Roussot, O., Said, F., Schwarzenboeck, A., Testor, P., Van Baelen, J., Vincendon, B., Aran, M., and Tamayo, J.: HyMeX-SOP1: The Field Campaign Dedicated to Heavy Precipitation and Flash Flooding in the Northwestern Mediterranean, B. Am. Meteorol. Soc., 95, 1083–1100, https://doi.org/10.1175/BAMS-D-12-00244.1, 2014.

Estaque, T., Richaume, J., Bianchimani, O., Schull, Q., Mérigot, B., Bensoussan, N., Sartoretto, S., Monfort, T., Basthard-Bogain, S., Fargetton, M., Gatti, G., Barth, L., Cheminée, A., and Garrabou, J.: Marine heatwaves on the rise: One of the strongest ever observed mass mortality event in temperate gorgonians, Global Change Biol., 29, 6159–6162, https://doi.org/10.1111/gcb.16931, 2023.

Estournel, C., Testor, P., Damien, P., D'Ortenzio, F., Marsaleix, P., Conan, P., Kessouri, F., Durrieu de Madron, X., Coppola, L., Lellouche, J. M., Belamari, S., Mortier, L., Ulses, C., Bouin, M. N., and Prieur, L.: High resolution modeling of dense water formation in the north-western Mediterranean during winter 2012–2013: Processes and budget, J. Geophys. Res.-Oceans, 121, 5367–5392, https://doi.org/10.1002/2016JC011935, 2016.

Estournel, C., Marsaleix, P., and Ulses, C.: A new assessment of the circulation of Atlantic and Intermediate Waters in the Eastern Mediterranean, Prog. Oceanogr., 198, 102673, https://doi.org/10.1016/j.pocean.2021.102673, 2021.

Faranda, D., Pascale, S., and Bulut, B.: Persistent anticyclonic conditions and climate change exacerbated the exceptional 2022 European-Mediterranean drought, Environ. Res. Lett., 18 034030, https://doi.org/10.1088/1748-9326/acbc37, 2023.

Fox-Kemper, B., Hewitt, H. T., Xiao, C., Aðalgeirsdóttir, G., Drijfhout, S. S., Edwards, T. L., Golledge, N. R., Hemer, M., Kopp, R. E., Krinner, G., Mix, A., Notz, D., Nowicki, S., Nurhati, I. S., Ruiz, L., Sallée, J.-B., Slangen, A. B. A., and Yu, Y.: Ocean, Cryosphere and Sea Level Change, in: Climate Change 2021: The Physical Science Basis, Contribution of Working Group I to the Sixth Assessment Report of the Intergovernmental Panel on Climate Change, edited by: Masson-Delmotte, V., Zhai, P., Pirani, A., Connors, S. L., Péan, C., Berger, S., Caud, N., Chen, Y., Goldfarb, L., Gomis, M. I., Huang, M., Leitzell, K., Lonnoy, E., Matthews, J. B. R., Maycock, T. K., Waterfield, T., Yelekçi, O., Yu, R., and Zhou, B., Cambridge University Press, Cambridge, UK and New York, NY, USA, 1211–1362, https://doi.org/10.1017/9781009157896.011, 2021.

Garrabou, J., Ledoux, J. B., Bensoussan, N., Gómez-Gras, D., and Linares, C.: Sliding Toward the Collapse of Mediterranean Coastal Marine Rocky Ecosystems, in: Ecosystem Collapse and Climate Change. Ecological Studies, vol. 241, edited by: Canadell, J. G. and Jackson, R. B., Springer, Cham, https://doi.org/10.1007/978-3-030-71330-0_11, 2021.

Garrabou, J., Gómez-Gras, D., Medrano, A., Cerrano, C., Ponti, M., Schlegel, R., Bensoussan, N., Turicchia, E., Sini, M., Gerovasileiou, V., Teixido, N., Mirasole, A., Tamburello, L., Cebrian, E., Rilov, G., Ledoux, J.-B., Souissi, J. B., Khamassi, F., Ghanem, R., Benabdi, M., Grimes, S., Ocaña, O., Bazairi, H., Hereu, B., Linares, C., Kersting, D. K., la Rovira, G., Ortega, J., Casals, D., Pagès-Escolà, M., Margarit, N., Capdevila, P., Verdura, J., Ramos, A., Izquierdo, A., Barbera, C., Rubio-Portillo, E., Anton, I., López-Sendino, P., Díaz, D., Vázquez-Luis, M., Duarte, C., Marbà, N., Aspillaga, E., Espinosa, F., Grech, D., Guala, I., Azzurro, E., Farina, S., Gambi, M. C., Chimienti, G., Montefalcone, M., Azzola, A., Pulido Mantas, T., Fraschetti, S., Ceccherelli, G., Kipson, S., Bakran-Petricioli, T., Petricioli, D., Jimenez, C., Katsanevakis, S., Kizilkaya, I. T., Kizilkaya, Z., Sartoretto, S., Rouanet, E., Ruitton, S., Comeau, S., Gattuso, J.-P., and Harmelin, J.-G.: Marine heatwaves drive recurrent mass mortalities in the Mediterranean Sea, Global Change Biol., 28, 5708–5725, https://doi.org/10.1111/gcb.16301, 2022.

Gómez-Gras, D., Linares, C., López-Sanz, A., Amate, R., Ledoux, J. B., Bensoussan, N., Drap, P., Bianchimani, O., Marschal, C., Torrents, O., Zuberer, F., Cebrian, E., Teixidó, N., Zabala, M., Kipson, S., Kersting, D. K., Montero-Serra, I., Pagès-Escolà , M., Medrano, A., Frleta-Valić, M., Dimarchopoulou, D., López-Sendino, P., and Garrabou, J.: Population collapse of habitat-forming species in the Mediterranean: a long-term study of gorgonian populations affected by recurrent marine heatwaves, P. Roy. Soc. B., 288, 202112384, https://doi.org/10.1098/rspb.2021.2384, 2021.

Glynn, P. W. and D'Croz, L.: Experimental evidence for high temperature stress as the cause of El Niño coincident coral mortality, Coral Reefs, 8, 181–191, https://doi.org/10.1007/BF00265009, 1990.

Grenier, M., Idan, T., Chevaldonné, P., and Perez, T.: Mediterranean marine keystone species on the brink of extinction, Global Change Biol., 29, 1681–1683, https://doi.org/10.1111/gcb.16597, 2023.

Guinaldo, T., Voldoire, A., Waldman, R., Saux Picart, S., and Roquet, H.: Response of the sea surface temperature to heatwaves during the France 2022 meteorological summer, Ocean Sci., 19, 629–647, https://doi.org/10.5194/os-19-629-2023, 2023.

Hughes, T., Kerry, J., Álvarez-Noriega, M., Álvarez-Romero, J. G., Anderson, K. D., Baird, A. H., Babcock, R. C., Beger, M., Bellwood, D. R., Berkelmans, R., Bridge, T. C., Butler, I. R., Byrne, M., Cantin, N. E., Comeau, S., Connolly, S. R., Cumming, G. S., Dalton, S. J., Diaz-Pulido, G., Mark Eakin, C., Figueira, W. F., Gilmour, J. P., Harrison, H. P., Heron, S. F., Hoey, A. S., Hobbs, J.-P. A., Hoogenboom, M., O., Kennedy, E. V., Kuo, C., Lough, J. M., Lowe, R. J., Liu, G., McCulloch, M. T., Malcolm, H. A., McWilliam, M. J., Pandolfi, J. M., Pears, R. J., Pratchett, M. S., Schoepf, V., Simpson, T., Skirving, W. J., Sommer, B., Torda, G., Wachenfeld, D. R., Willis, B. L., and Wilson, S. K.: Global warming and recurrent mass bleaching of corals, Nature, 543, 373–377, https://doi.org/10.1038/nature21707, 2017.

Jacquemont, J., Loiseau, C., Tornabene, L., and Claudet, J.: 3D ocean assessments reveal that fisheries reach deep but marine protection remains shallow, Nat. Commun., 15, 4027, https://doi.org/10.1038/s41467-024-47975-1, 2024.

Juza, M., Fernández-Mora, À., and Tintoré, J.: Sub-Regional Marine Heat Waves in the Mediterranean Sea From Observations: Long-Term Surface Changes, Sub-Surface and Coastal Responses, Front. Mar. Sci., 9, 785771, https://doi.org/10.3389/fmars.2022.785771, 2022.

Lejeusne, C., Chevaldonné, P., Pergent-Martini, C., Boudouresque, C. F., and Pérez, T. : Climate change effects on a miniature ocean: the highly diverse, highly impacted Mediterranean Sea, Trends Ecol. Evol., 25, 250–260, https://doi.org/10.1016/j.tree.2009.10.009, 2010.

Marsaleix, P.: SYMPHONIE model Sources, Zenodo [code], https://doi.org/10.5281/zenodo.13774747, 2024.

Marsaleix, P., Auclair, F., and Estournel, C.: Considerations on Open Boundary Conditions for Regional and Coastal Ocean Models, J. Atmos. Ocean. Tech., 23, 1604–1613, https://doi.org/10.1175/JTECH1930.1, 2006.

Marsaleix, P., Auclair, F., Floor, J. W., Herrmann, M. J., Estournel, C., Pairaud, I., and Ulses, C.: Energy conservation issues in sigma-coordinate free-surface ocean models, Ocean Model., 20, 61–89, https://doi.org/10.1016/j.ocemod.2007.07.005, 2008.

Martinez, J., Leonelli, F. E., García-Ladona, E., Garrabou, J., Kersting, D. K., Bensoussan, N., and Pisano, A.: Evolution of marine heatwaves in warming seas: the Mediterranean Sea case study, Front. Mar. Sci., 10, 1193164, https://doi.org/10.3389/fmars.2023.1193164, 2023.

Marullo, S., Serva, F., Iacono, R., Napolitano, E., di Sarra, A., Meloni, D., Monteleone, F., Sferlazzo, D., De Silvestri, L., de Toma, V., Pisano, A., Bellacicco, M., Landolfi, A., Organelli, E., Yang, C., and Santoleri, R.: Record-breaking persistence of the 2022/23 marine heatwave in the Mediterranean Sea, Environ. Res. Lett., 18, 114041, https://doi.org/10.1088/1748-9326/ad02ae, 2023.

Mikolajczak, G., Ulses, C., Estournel, C., Bourrin, F., Pairaud, I., Martín, J., Puig, P., Durrieu de Madron, X., Leredde, Y., and Marsaleix, P.: Impact of storms on residence times and export of coastal waters during a mild fall/winter period in the Gulf of Lion, Cont. Shelf Res., 207, 104192, https://doi.org/10.1016/j.csr.2020.104192, 2020.

Millot, C.: The gulf of Lions' hydrodynamics, Cont. Shelf Res., 10, 885–894, 1990.

Obermann-Hellhund, A., Conte, D., Somot, S., Torma, C. Z., and Ahrens, B.: Mistral and Tramontane wind systems in climate simulations from 1950 to 2100, Clim. Dynam., 50, 693–703, https://doi.org/10.1007/s00382-017-3635-8, 2018.

Odic, R., Bensoussan, N., Pinazo, C., Taupier-Letage, I., and Rossi, V.: Sporadic wind-driven upwelling / downwelling and associated cooling/warming along Northwestern Mediterranean coastlines, Cont. Shelf Res., 250, 104843, https://doi.org/10.1016/j.csr.2022.104843, 2022.

Pairaud, I. L., Bensoussan, N., Garreau, P., Faure, V., and Garrabou, J.: Impacts of climate change on coastal benthic ecosystems: assessing the current risk of mortality outbreaks associated with thermal stress in NW Mediterranean coastal areas, Ocean Dynam., 64, 103–115, https://doi.org/10.1007/s10236-013-0661-x, 2014.

Pastor, F. and Khodayar Pardo, S.: Marine heat waves: Characterizing a major climate impact in the Mediterranean, Sci. Total Environ., 861, 160621, https://doi.org/10.1016/j.scitotenv.2022.160621, 2023.

Pastor, F., Valiente, J. A., and Khodayar, S.: A Warming Mediterranean: 38 Years of Increasing Sea Surface Temperature, Remote Sens., 12, 2687, https://doi.org/10.3390/rs12172687, 2020.

Ponti, M., Perlini, R. A., Ventra, V., Grech, D., Abbiati, M., and Cerrano, C.: Ecological Shifts in Mediterranean Coralligenous Assemblages Related to Gorgonian Forest Loss, PLoS ONE, 9, e102782, https://doi.org/10.1371/journal.pone.0102782, 2014.

Ross, O. N., Fraysse, M., Pinazo, C., and Pairaud, I.: Impact of an intrusion by the Northern Current on the biogeochemistry in the eastern Gulf of Lion, NW Mediterranean, Estuar. Coast. Shelf Sci., 170, 1–9, https://doi.org/10.1016/j.ecss.2015.12.022, 2016.

Sartoretto, S., Ledoux, J. B., Gueret, E., Guillemain, D., Ravel, C., Moirand, L., and Aurelle, D.: Ecological and genomic characterization of a remarkable natural heritage: a mesophotic 'giant'

Paramuricea clavata forest, Mar. Ecol. Prog. Ser., 728, 85–101, https://doi.org/10.3354/meps14427, 2023.

Schaeffer, A., Sen Gupta, A., and Roughan, M.: Seasonal stratification and complex local dynamics control the subsurface structure of marine heatwaves in Eastern Australian coastal waters, Commun. Earth Environ., 4, 304, https://doi.org/10.1038/s43247-023-00966-4, 2023.

Simon, A., Plecha, S. M., Russo, A., Teles-Machado, A., Donat, M. G., Auger, P.-A., and Trigo, R. M.: Hot and cold marine extreme events in the Mediterranean over the period 1982–2021, Front. Mar. Sci., 9, 892201, https://doi.org/10.3389/fmars.2022.892201, 2022.

T-MedNet: Tracking climate change effects in the Mediterranean, https://t-mednet.org/ (last access: 16 July 2025), 2025.

Ulses, C., Estournel, C., Bonnin, J., Durrieu de Madron, X., and Marsaleix, P.: Impact of storms and dense water cascading on shelf-slope exchanges in the Gulf of Lion (NW Mediterranean), J. Geophys. Res., 113, C02010, https://doi.org/10.1029/2006JC003795, 2008.

Verdura, J., Linares, C., Ballesteros, E., Coma, R., Uriz, M. J., Bensoussan, N., and Cebrian, E.: Biodiversity loss in a Mediterranean ecosystem due to an extreme warming event unveils the role of an engineering gorgonian species, Sci. Rep., 9, 5911, https://doi.org/10.1038/s41598-019-41929-0, 2019.